

# Event anisotropy $v_2$ in Au+Au collisions at $\sqrt{s_{NN}} = 7.7 - 62.4$ GeV with STAR

Shusu Shi<sup>a,b</sup> (for the STAR Collaboration)<sup>1</sup>

<sup>a</sup>*Institute of Particle Physics, Huazhong Normal University, Wuhan, Hubei, 430079, China*

<sup>b</sup>*Key Laboratory of Quark and Lepton Physics (MOE) and Institute of Particle Physics, Central China Normal University, Wuhan 430079, China*

---

## Abstract

We present the  $v_2$  measurement at midrapidity from Au+Au collisions at  $\sqrt{s_{NN}} = 7.7, 11.5, 19.6, 27, 39$  and  $62.4$  GeV for inclusive charged hadrons and identified hadrons ( $\pi^\pm, K^\pm, K_S^0, p, \bar{p}, \phi, \Lambda, \bar{\Lambda}, \Xi^-, \bar{\Xi}^+, \Omega^-, \bar{\Omega}^+$ ) up to  $4$  GeV/ $c$  in  $p_T$ . The beam energy and centrality dependence of charged hadron  $v_2$  are presented with comparison to higher energies at RHIC and LHC. The identified hadron  $v_2$  are used to discuss the NCQ scaling for different beam energies. Significant difference in  $v_2(p_T)$  is observed between particles and corresponding anti-particles for  $\sqrt{s_{NN}} < 39$  GeV. These differences are more pronounced for baryons compared to mesons and they increase with decreasing energy.

---

## 1. Introduction

Searching for the phase boundary in the Quantum ChromoDynamics (QCD) phase diagram is one of the main motivations of the Beam Energy Scan (BES) program at RHIC. The elliptic flow ( $v_2$ ) could be used as a powerful tool [1], because of the sensitivity of underlying dynamics in the early stage of the collisions. The Number of Constituent Quark (NCQ) scaling in the top energy collisions at RHIC ( $\sqrt{s_{NN}} = 200$  GeV) indicates the collectivity has been built up in the partonic level [2, 3]. Recently, the similar NCQ scaling of multi-strange hadrons,  $\phi$  and  $\Omega$ , which are less sensitive to the late hadronic interactions, provides the clear evidence of partonic collectivity [4]. An energy dependence study based on A Multi-Phase Transport (AMPT) model indicates the NCQ scaling is related to the degrees of freedom in the system [5]. If the partonic degree of freedom is included in the AMPT model, the NCQ scaling (including multi-strange hadrons) could be observed; whereas the NCQ scaling is broken in the case of including only hadronic degrees of freedom. The BES data offer us the opportunity to investigate the QCD phase boundary with  $v_2$  measurements. In this paper, we present the  $v_2$  results from the STAR experiment in Au+Au collisions at  $\sqrt{s_{NN}} = 7.7 - 62.4$  GeV. The particle identification for  $\pi^\pm, K^\pm$  and  $p$  ( $\bar{p}$ ) is achieved via the energy loss in the Time Projection Chamber (TPC) [6] and the time-of-flight information from the multi-gap resistive plate chamber detector [7]. Strange and multi-strange hadrons are reconstructed with the decay channels:  $K_S^0 \rightarrow \pi^+ + \pi^-$ ,  $\phi \rightarrow K^+ + K^-$ ,  $\Lambda \rightarrow p + \pi^-$  ( $\bar{\Lambda} \rightarrow \bar{p} + \pi^+$ ),  $\Xi^- \rightarrow \Lambda + \pi^-$  ( $\bar{\Xi}^+ \rightarrow \bar{\Lambda} + \pi^+$ ) and  $\Omega^- \rightarrow \Lambda + K^-$  ( $\bar{\Omega}^+ \rightarrow \bar{\Lambda} + K^+$ ). The event plane method [8] and cumulant method [9, 10] are used for the  $v_2$  measurement.

---

<sup>1</sup>A list of members of the STAR Collaboration and acknowledgements can be found at the end of this issue.

## 2. Results and Discussions

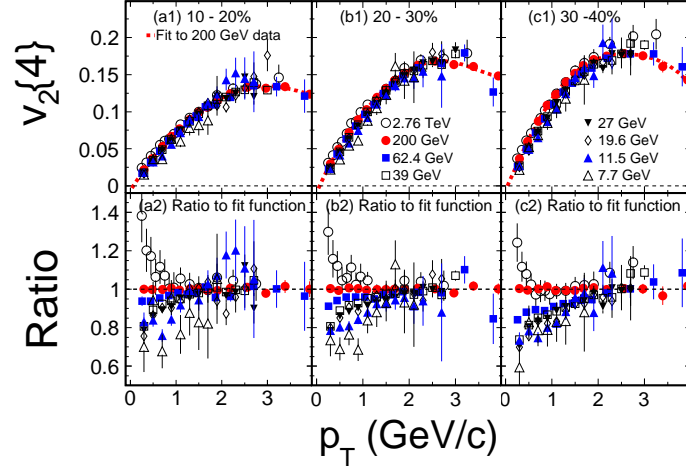


Figure 1: (Color online) The top panels show  $v_2\{4\}$  vs.  $p_T$  for charged hadrons at midrapidity for various collision energies ( $\sqrt{s_{NN}} = 7.7$  GeV to 2.76 TeV). The results for  $\sqrt{s_{NN}} = 7.7$  to 200 GeV are for Au+Au collisions and those for 2.76 TeV are for Pb + Pb collisions [11]. The dashed curves show the fifth order polynomial fits to the results from Au+Au collisions at  $\sqrt{s_{NN}} = 200$  GeV. The bottom panels show the ratio of  $v_2\{4\}$  vs.  $p_T$  for all  $\sqrt{s_{NN}}$  with respect to the fit curve. The results are shown for three collision centrality classes: 10 – 20% (a1), 20 – 30% (b1) and 30 – 40% (c1). Error bars are shown only for the statistical uncertainties respectively.

Figure 1 [11] shows the transverse momentum ( $p_T$ ) dependence of  $v_2\{4\}$  from  $\sqrt{s_{NN}} = 7.7$  GeV to 2.76 TeV in 10 – 20% (a1), 20 – 30% (b1) and 30 – 40% (c1) centrality bins. The ALICE results in Pb + Pb collisions at  $\sqrt{s_{NN}} = 2.76$  TeV are taken from Ref. [12]. The 200 GeV data is empirically fit by a fifth order polynomial function. For comparison, the  $v_2$  from other energies are divided by the fit and shown in the lower panels of Fig. 1. For  $p_T$  below 2 GeV/c, the  $v_2$  values rise with increasing collision energy. Beyond  $p_T = 2$  GeV/c the  $v_2$  results show comparable values within statistical errors. The increase of  $v_2(p_T)$  as a function of energy could be due to the change of chemical composition from low to high energies and/or larger collectivity at higher collision energy.

Figure 2 shows the  $p_T$  independent difference in  $v_2$  between particles and their corresponding anti-particles. The data of collisions at  $\sqrt{s_{NN}} = 19.6$  and 27 GeV is new since Quark Matter 2011 [13]. The  $\eta$ -sub event plane method is used for the measurement. In this method, one defines the flow vector for each particle based on particles measured in the opposite hemisphere in pseudorapidity ( $\eta$ ). An  $\eta$  gap of  $|\eta| < 0.05$  is used between negative/positive  $\eta$  sub-event to reduce the non-flow effects of short  $\eta$  range correlations by enlarging the separation between the correlated particles.  $v_2(X) - v_2(\bar{X})$  ( $\Delta v_2$ ) represents the average values of the difference in  $v_2$  between particles and corresponding anti-particles over the measured  $p_T$  range. The dashed lines in the Fig. 2 are fits with the function:  $f_{\Delta v_2}(\sqrt{s_{NN}}) = a\sqrt{s_{NN}}^{-b} + c$ . A monotonic increase of  $\Delta v_2$  with decreasing collision energy is observed and the slope of the difference increases towards lowers energies. The difference is more pronounced for baryons compared to mesons. The

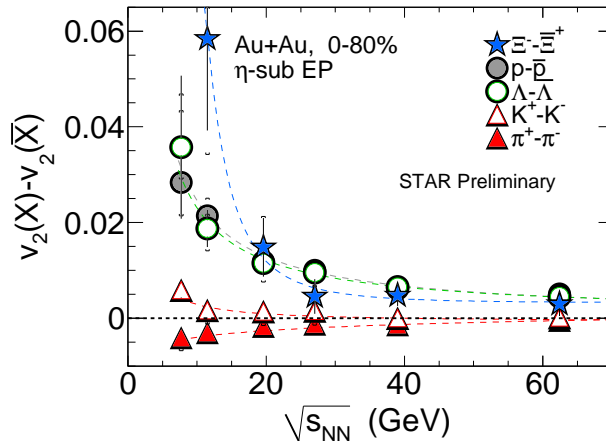


Figure 2: (Color online) The difference in  $v_2$  between particles and their corresponding anti-particles ( $v_2(X) - v_2(\bar{X})$ ) as a function of beam energy in Au+Au collisions (0-80%). The statistical and systematic uncertainties are shown by vertical line and cap respectively. The dashed lines in the plot are fits with the equation described in the text.

observed difference in  $v_2$  reflects that the particles vs. anti-particles could not fit into the NCQ scaling. The breaking of NCQ scaling between particles and anti-particles indicates the contributions from hadronic interactions increase in the system evolution with decreasing collision energy. The energy dependence of  $\Delta v_2$  could be qualitatively reproduced by the baryon transport effect [14] or hadronic potential effect [15]. So far theoretical calculations fail to quantitatively reproduce the measured  $v_2$  difference and none of the calculations could explain the correct order of particles.

Figure 3 shows the  $v_2$  as a function of transverse mass ( $m_T - m_0$ ) for the selected particles for all six collision energies. In the top energy ( $\sqrt{s_{NN}} = 200$  GeV) collisions, a clear splitting in  $v_2$  between baryons and mesons is observed for  $m_T - m_0 > 1$  GeV/ $c^2$ . The splitting between baryons and mesons suggest the system created in the collisions is sensitive to the quark degree of freedom. The selected particles show a similar splitting for collision energy  $\geq 39$  GeV. The baryon and meson groups become closer to each other at all lower energies. At  $\sqrt{s_{NN}} = 11.5$  GeV, the splitting between baryons and mesons is almost gone. The clear trend, a decreasing baryon-meson splitting of  $v_2(m_T - m_0)$  beyond  $m_T - m_0 > 1$  GeV/ $c^2$  indicates the hadronic interactions become more important in the lower collision energies.

### 3. Summary

In summary, we present the  $v_2$  measurements for charged and identified hadrons in Au+Au collisions at  $\sqrt{s_{NN}} = 7.7 - 62.4$  GeV. The comparison with Au+Au collisions at higher energies at RHIC ( $\sqrt{s_{NN}} = 62.4$  and 200 GeV) and at LHC (Pb + Pb collisions at  $\sqrt{s_{NN}} = 2.76$  TeV) shows that the  $v_2\{4\}$  values at low  $p_T$  ( $p_T < 2.0$  GeV/ $c$ ) increase with increase in collision energy. The baryon and anti-baryon  $v_2$  show significant difference for  $\sqrt{s_{NN}} < 39$  GeV. The difference of  $v_2$  between particles and corresponding anti-particles (pions, kaons, protons,  $\Lambda$ s and  $\Xi$ s) increases

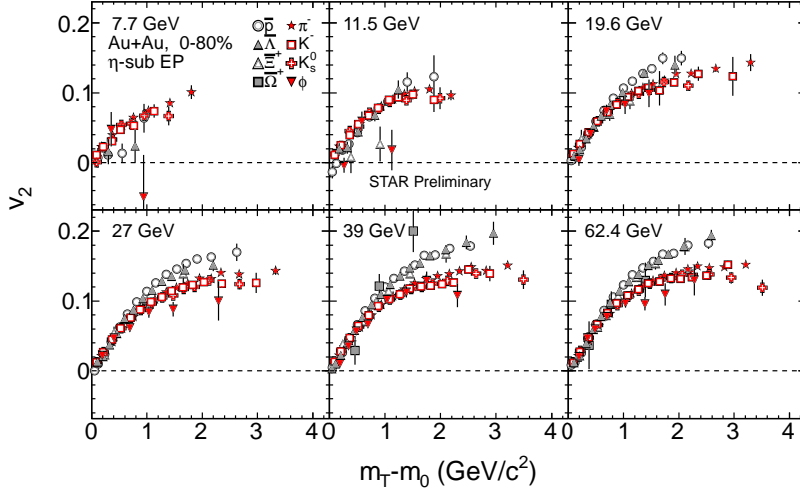


Figure 3: (Color online) The elliptic flow ( $v_2$ ) as a function of transverse mass ( $m_T - m_0$ ) for the selected particles in Au+Au collisions (0-80%) at  $\sqrt{s_{NN}} = 7.7, 11.5, 19.6, 27, 39$  and  $62.4$  GeV. Error bars are shown only for the statistical uncertainties.

with decreasing the beam energy. The baryon-meson splitting of  $v_2(m_T - m_0)$  beyond  $m_T - m_0 > 1$   $\text{GeV}/c^2$  becomes smaller in the lower collisions energy and is almost gone in collisions at  $\sqrt{s_{NN}} = 11.5$  GeV. Experimental data indicate that the hadronic interactions become more important at the lower beam energy.

#### 4. Acknowledgments

This work was supported in part by the National Natural Science Foundation of China under grant No. 11105060, 10775060, 11135011, 11221504 and self determined research funds of CCNU from the colleges' basic research and operation of MOE.

#### References

- [1] S. A. Voloshin, A. M. Poskanzer and R. Snellings, arXiv:0809.2949.
- [2] J. Adams *et al.* (STAR Collaboration), Phys. Rev. Lett. **92**, 052302 (2004).
- [3] B. I. Abelev *et al.*, (STAR Collaboration), Phys. Rev. C **81**, 044902 (2010).
- [4] S. S. Shi (for the STAR collaboration), Nucl. Phys. A **830**, 187c (2009); Nucl. Phys. A **862-863**, 263 (2011).
- [5] F. Liu, K.J. Wu, and N. Xu, J. Phys. G **37** 094029(2010).
- [6] K. H. Ackermann *et al.* (STAR Collaboration), Nucl. Instrum. Methods A **499**, 624 (2003).
- [7] W. J. Llope (STAR TOF Group), Nucl. Instr. and Meth. B **241**, 306 (2005).
- [8] A. M. Poskanzer and S. A. Voloshin, Phys. Rev. C **58** 1671 (1998).
- [9] N. Borghini, P. M. Dinh, and J.-Y. Ollitrault, Phys. Rev. C **63**, 054906 (2001).
- [10] A. Bilandzic, R. Snellings and S. Voloshin, Phys. Rev. C **83**, 044913 (2011).
- [11] L. Adamczyk *et al.*, (STAR Collaboration), arXiv:1206.5528.
- [12] K. Aamodt *et al.* (ALICE Collaboration), Phys. Rev. Lett. **105**, 252302 (2010).
- [13] A. Schmah (for the STAR collaboration), J. Phys. G **38** 124049 (2011).
- [14] J. Dunlop, M.A. Lisa and P. Sorensen, Phys. Rev. C **84**, 044914 (2011).
- [15] J. Xu *et al.*, Phys. Rev. C **85**, 041901 (2012).